3-1-1995

ITS Wireless Narrowband Digital Communication Architecture Design Report

Michael P. Fitz,
Purdue University School of Electrical Engineering

Jimm Grirnm
Purdue University School of Electrical Engineering

Tim Magnusen
Purdue University School of Electrical Engineering

Wen Yi Kuo
Purdue University School of Electrical Engineering

Tai Ann Chen
Purdue University School of Electrical Engineering

See next page for additional authors

Authors
Michael P. Fitz,; Jimm Grirnm; Tim Magnusen; Wen Yi Kuo; Tai Ann Chen; Jerome Gansman; and Lance Bodnar

ITS Wireless Narrowband Digital Communication Architecture Design Report

Michael P. Fitz
Jimm Grimm
Tim Magnusen
Dr. Wen-yi Kuo
Tai-ann Chen
Jerome Gansman
Lance Bodnar

TR-EE 95-6
March 1995

School of Electrical Engineering
Purdue University
West Lafayette, Indiana 47907-1285

ITS Wireless Narrowband Digital Communication Architecture Design Report

Communications Research Laboratory

Professor Michael P. Fitz, PI
Jimm Grimm
Tim Magnusen
Dr. Wen-yi Kuo
Tai-ann Chen
Jerome Gansman
Lance Bodnar

School of Electrical Engineering
1285 Electrical Engineering Building
Purdue University
West Lafayette, IN 47907-1285

This project is funded by the ITS-IDEA program through the National Academy of Sciences under the Department of Transportation Agreement No. DTFH61-92-X-0026.

Table of Contents

I. Abstract

This report provides a detailed overview of the Intelligent Transportation System (ITS) narrowband digital communicator project. The project is the building and field testing of a high performance modem architecture on the 220MHz radio channels allocated to ITS. This architecture will provide greater than 12kbits/s transmission rate by using state of the art techniques to develop a new paradigm in bandwidth efficient land mobile communications. The main goals are to develop a recursive model based optimum demodulator and to implement the architecture necessary for actual field tests. The modulation scheme optimizes the use of transmitter antenna diversity, forward error control coding, pilot symbol assisted modulation, and the statistical characteristics of the received signal.

An overview of the entire communication system as well as a discussion of every subsystem is included in this report. Theoretical issues such as error correction coding, modulation format, transmitter diversity, and pilot symbol assisted demodulation are investigated. Implementation issues such as the frame structure, synchronization, link budgets, and the radio frequency transmitter and receiver are also addressed.

The resulting system will achieve 3 bits/Hz bandwidth efficiency with a bit error probability of 10^{-5} using wireless land mobile radio communication. The design is very flexible and can accommodate a wide variety of digitally modulated signals for many applications. The architecture will provide the framework for testing this and future algorithms in an actual urban environment.

II. Overview

The goal of this project is the construction and field test of a high performance narrowband land mobile communications physical layer architecture. The project concentrates on the infrastructure to mobile communications link and seeks to achieve a greater than 3 bits/s/Hz raw data transmission bandwidth efficiency while maintaining significant range. This goal will be achieved by utilizing quadrature amplitude modulation (QAM) having a large number of bits per symbol, multiple antennas for diversity transmission, and sophisticated signal processing techniques optimized for the wireless land mobile communications channel. Figure 1 is the overall block diagram of the system being constructed in this project. The data generation system (DGS) and the data recovery system (DRS) are constructed solely for the field test of the communication system. The DGS and DRS generate and decode the test sequences which allow the units to detect proper synchronization and make an assessment of the resulting bit error rate. The radio frequency (RF) transmitter and receiver provide both the frequency conversion and amplification necessary to produce the 220MHz communication link. The sophistication of this project resides in the baseband modulators and demodulators. These units provide narrowband digitally modulated signals and the demodulation architectures optimized for wireless land mobile cocnmunication.

Fig. 1. Narrowband digital communicator overall block diagram

III. Data Generation and Recovery Systems

A. Purpose

The data generation system (DGS) and data recovery systems (DRS) provide a method of generating known test data and calculating the resulting bit error rate.

B. Design

The DGS generates data in two frames. The first frame, referred to as the unique word (UW), is used to verify that synchronization has been established. If the UW is not detected in the proper :places, then it is assumed that synchronization has been lost and the received data is bad, thus the probability of bit error is not calculated for this data. The second :frame, referred to as the user frame (UF), consists of the transmitted data. These two fracnes are repeated indefinitely. In a real system, each user frame will contain new data, but for testing purposes the same data :sequence is used in each user frame. This test data is pseudo randomly generated using a maximal length shift register with sufficient length to achieve the desired channel efficiency.

The DRS reads in all information received. It then scans the received data for the first UW. When the DRS locates the first UW, it then scans for the UW of the next frame. If both UW are

identified, the data between them is assumed to be the UF and the number of errors in the received signal are counted. If the second UW is not identified in the proper place, the DRS assumes synchronization was lost and begins searching the data for a new UW to detect the start of a new frame.

IV. RF Transmitter and Receiver

A. Purpose

The RF transmitter and receiver units are being procured from outside the University and will provide the frequency conversion, filtering, and amplification necessary to produce a 220MHz digitally modulated carrier. The actual units are general purpose units capable of covering a much larger frequency range than this project requires. These units are being purchased with matching funds obtained from the School of Electrical Engineering, AT&T Foundation, and the National Science Foundation.

B. Design

Both the transmitter and receiver units will employ standard designs. Figure 2 shows the transmitter unit (TU). The TU will be especially simple since high output power is not required. Demonstration of the waveforms and architecture in real wireless channels is the purpose of the field testing and this can be accomplished without high power amplifiers. High power amplifiers are traditionally where a majority of the distortion is produced in land mobile communication links. Linearized high power amplifiers will be considered in the next stage of the development. The external local oscillator will be supplied by Hewlett Packard test equipment available within the Communications Research Laboratory at Purdue University. Three RF transmitters will be used to implement the transmitter diversity scheme.

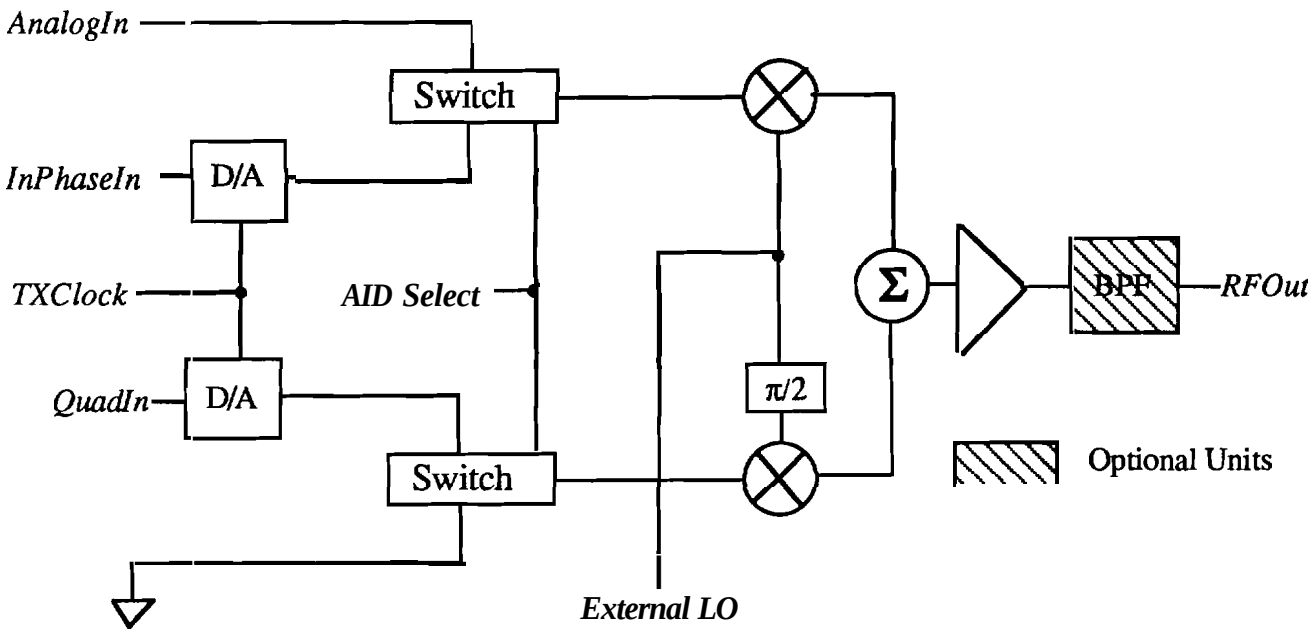

Fig. 2. Transmitter unit block diagram.

The receiver unit (RU) will also use a standard design which is seen in Fig. 3. The minimum detectable input signal power level will be -120dBm which will enable us to obtain significant range without a large transmitted power level. As in the TU, the external local oscillator will be provided by Hewlett Packard test equipment. The digital outputs can either be processed by a digital signal processor or loaded onto the computer network. Once on the network software implementations of the baseband demodulator can be tested and verified.

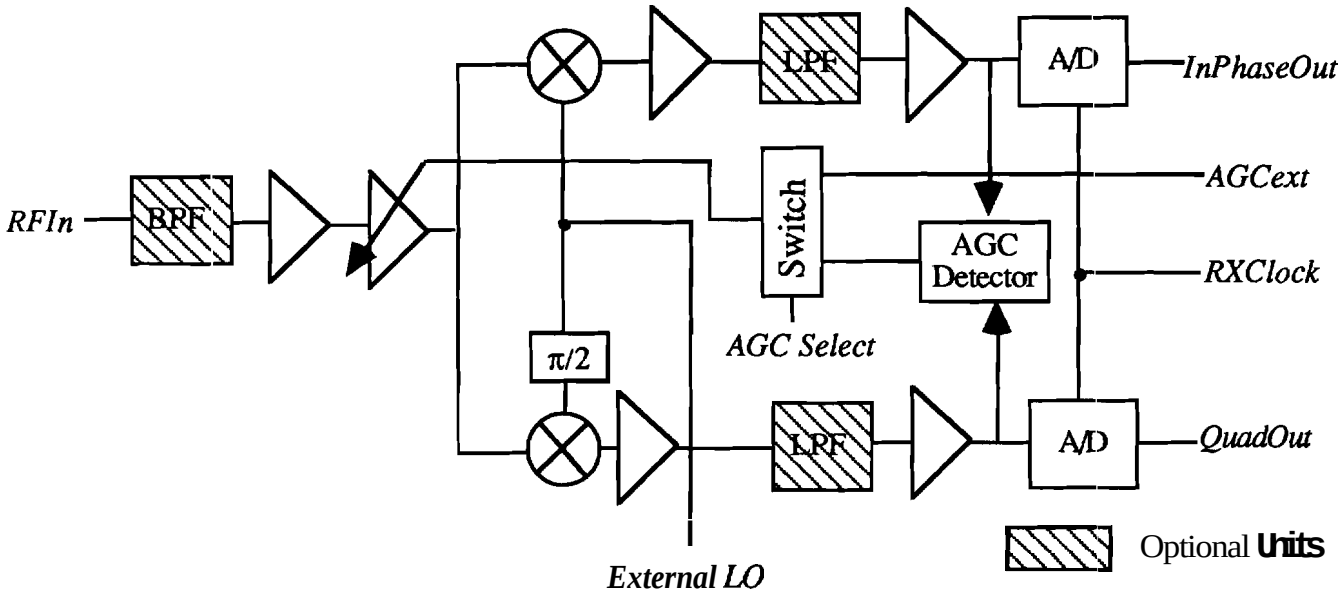

Fig. 3. Receiver unit block diagram

V. Modulator

A. Purpose

The modulator converts the data to a format suitable for transmission over the fading channel. Since the transmitter employs a linear amplifier, linear modulation schemes may be used, and QAM was chosen because of its high bandwidth efficiency. The goal of this project is to achieve 3 bits/Hz, but to compensate for losses in filtering, coding :redundancy, and synchronization, the modulation scheme of choice will need to have better than 3 bits/Hz efficiency. It is well known that 16QAM has the potential to achieve 4 bits/Hz, but few existing 16QAM systems surpass 2 bits/Hz for data transmission. Therefore, 16QAM will be used in this system for troubleshooting and to compare performance to prior results, and the final modulation will be 64QAM or 128Cross.

A block diagram of the modulator is shown in Figure 4. The input bits from the DGS are converted to m bit symbols and coded using a block code. Next the symbols are: interleaved so at the decoder, when the symbols are deinterleaved, the fading on each symbol of the codewords will be uncorrelated. The symbols are then mapped to a QAM constellation. The pilot symbols are mapped to a phase shift keying (PSK) constellation to help distinguish the pilot symbols from the data symbols at the receiver. A pilot symbol is inserted after every N_p-1 data symbols, and all symbols are shaped by the same pulse shaping filter, which must have a bandwidth of 4kHz

and minimize the inter-symbol interference (ISI). The signal is then modulated to an intermediate frequency (IF) of 10kHz and passed to the RF transmitter.

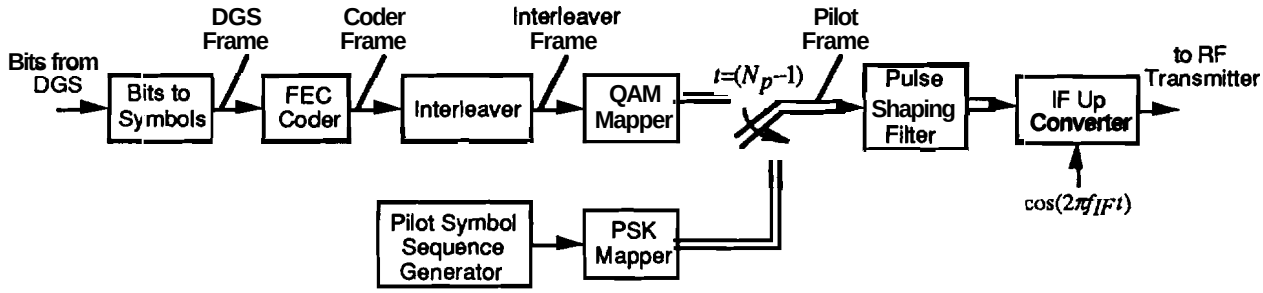

Fig. 4. Modulator block diagram

The entire modulator including the DGS is implemented in a Motorola 56002 DSP board, and the IF modulated signal is passed to the RF transmitter through a D/A board. This DSP chip has sufficient processing power to meet all the requirements, and allows modifications to be made to the system relatively easily.

B. Coding Strategies

The coding strategies will employ standard block coding techniques generalized to larger modulation alphabets. As our project communication performance is bounded by the times when the link is stationary and in a deep fade (see Section VII-A) the coding strategies will be design for this case. A diversity level of 3 which translates into a Hamming distance requirement of 3 for the codes is the design criteria needed to achieve good performance. The complexity of soft decision decoding is $O(M^N)$ where M is the constellation size and N is the length of the code. Also, long codewords tend to reduce the advantages of antenna diversity when a small number of antennas is used. Consequently short codewords are desired. Fortunately very simple linear block codes can give a Hamming distance equal to 3 [1]. Linear block codes are normally taken to have binary values but the generalization to M-ary modulations is trivial. Table 1 is a list of the codes that will be considered for this project. The first code is the one for which much of the antenna diversity analysis has been accomplished (see Section VII-E) and it will be used to troubleshoot the baseband signal processing, compare to the analysis, and troubleshoot the entire communication architecture. The progressively more efficient architectures will be implemented as field testing proceeds.

Table 1. Project Coding Strategies

Rate, ~(Code Length)	Constellation (Bits/symbol)	Efficiency
1/3 (3)	16QAM (4)	1.3
1/3 (3)	64QAM (6)	2.0
2/5 (5)	32Cross (5)	2.0
2/5 (5)	64QAM (6)	2.4
4/7 (7)	32Cross (5)	2.8
4/7 (7)	64QAM (6)	3.43
4/7 (7)	128Cross (7)	4.0

C. Frame Structure

The frame structure for the transmitter must be able to support forward error control (FEC) coding, interleaving, pilot symbols and the UW. It is required that the frame at the output of each block of the modulator (in Figure 4) contains an integer number of symbols, so the following analysis examines each frame structure in detail.

C-1. DGS Frame

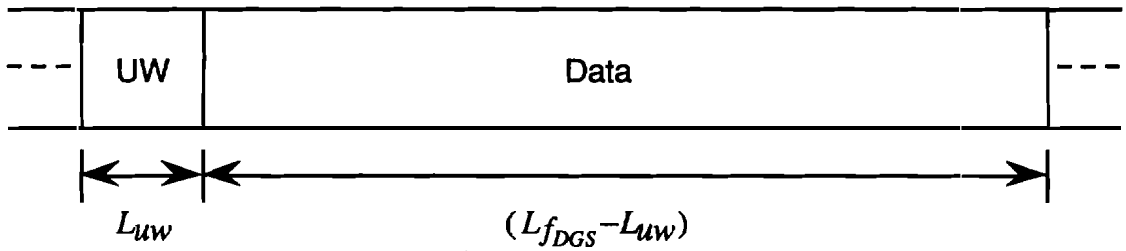

Fig. 5. DGS Frame

The frame at the output of the DGS is shown in Fig. 5. All lengths in this and the following figures are measured in symbols. In the most general case, the length of tht: UW L_{uw} is not necessarily an integer, although the DGS frame length $L_{f_{DGS}}$ must be an integer.

C-2. Coded Frame

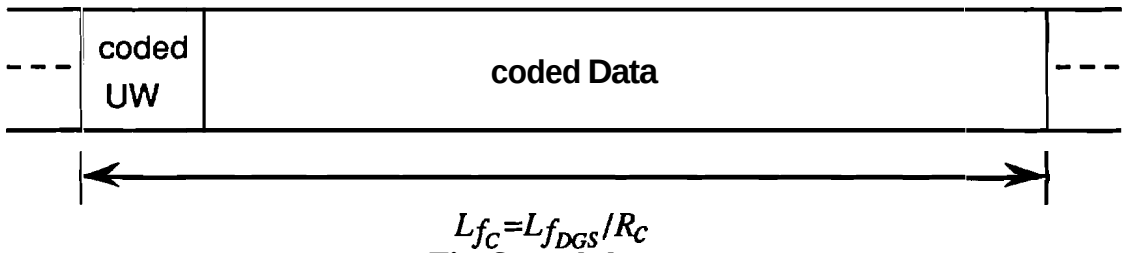

Fig. 6. Coded Frame

Figure 6 shows that after the output of the DGS is passed through a rate R_C coder the frame length becomes $Lf_C=Lf_{DGS}/R_C$. The code rate R_C is equal to the number of input symbols to the coder divided by the number of output symbols from the coder; $R_C=L_{Ci}/L_{CO}$. The requirement that the frame must contain an integer number of symbols implies that $L_{f_{DGS}}/L_{Ci}$ must be an integer. Since the UW and the data are both being coded in the same fashion it is not necessary for L_{uw} to be an integer. However, if the UW was to remain uncoded, L_{uw} would need to be an integer.

C-3. Interleaver Frame

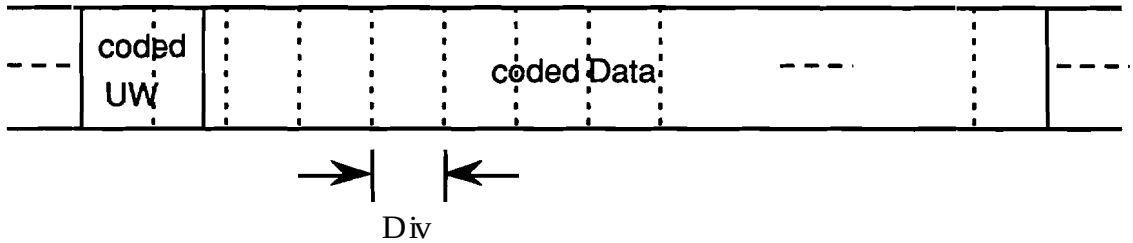

Fig. 7. Interleaver Frame

The interleaver does not change the data rate, so the interleaver frame in Fig. 7 has length $L_{f_I}=L_{f_C}$. The interleaver block size must be $D_{iv}\times L_{co}$ to achieve the desired interleaving, so the interleaver block size is $D_{iv}L_{co}$. For the interleaving to be uniform over the codewords, D_{iv}/L_{co} must be an integer. It would also be convenient to have: $L_{f_I}/(D_{iv}L_{co})$ be an integer in order to have an integer number of interleaver blocks in one frame. The UW and the data are both interleaved.

C-4. Pilot Symbol Frame

Pilot symbols are inserted after every N_p-1 data symbols, resulting in pilot symbols spaced N_p symbols apart. An example of this is shown in Figures 8 and 9 for N_p=6, with arrows indicating pilot symbol insertion points.

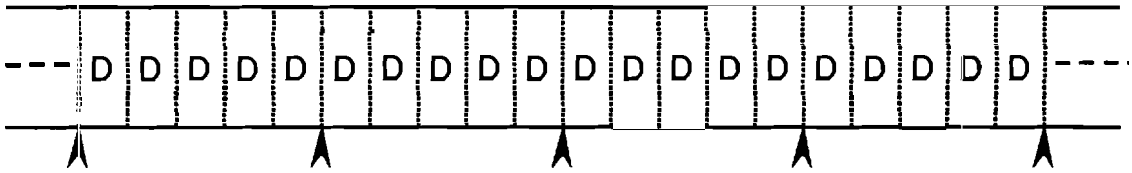

Fig. 8. Data stream before pilot insertion

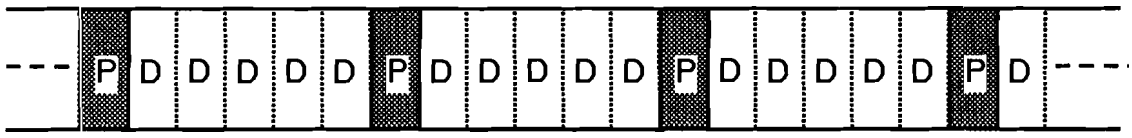

Fig. 9. Data stream after pilot insertion

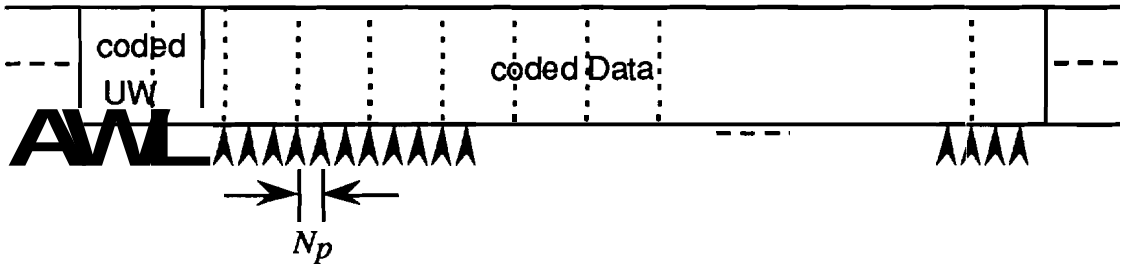

Fig. 10. Pilot Symbol Frame

In this final frame, shown in Fig. 10, there are $L_{f_{PS}}=L_{f_I}(1+1/(N_p-1))$ symbols. For this to be an integer, $L_{f_I}/(N_p-1)$ must be an integer.

Inserting the same pilot symbol every time introduces a nonzero mean and a periodic component to the data stream. To reduce these effects a periodic sequence of pilot symbols with period T_p is used. The longer the period of the sequence, the better the correlation peak of the synchronization system will be.

All of the frame synchronization for the system is obtained through the pilot symbols. The coder is synchronized to the pilot symbols by requiring $(N_p-1)/L_{CO}$ to be an integer, and transmitting a code block immediately following the pilot symbol insertion. The interleaver block $D_{iv}L_{CO}$ is larger than N_p-1, so the interleaver is synchronized to the pilot "superframe" (the entire sequence of T_p pilot symbols). To this end, it is required that $(N_p-1)T_p/(D_{iv}L_{CO})$ be an integer.

D. Modulation Format

As a result of the constraints imposed by the frame structure, and additional constraints that will be addressed later in this report, the following parameters were chosen for the modulation format for the baseline code rate R_C=1/3 system:

The pilot symbol insertion interval N_p was chosen to be 10 to achieve high oversampling of the noise process and some noise tolerance. Sequences for PSK with a period of 12 were discovered.that had good autocorrelation properties, so T_p was chosen to be 12. The remaining frame structure constraints were satisfied by choosing D_{iv}=36, thus frequency offset f_O=34.3Hz. This results in $D_{iv}L_{CO}$=108, so we set L_{f_C}=11$D_{iv}L_{CO}$=1188 symbols, thus for R_C=113, $L_{f_{DGS}}$=396. A similar procedure may be used for other code rates.

The bandwidth efficiency of the modulation is

$$\eta=mR_C\frac{R_S}{4kHz}\frac{(N_p-1)}{N_p}\text{ bits/Hz},$$

so the efficiency of this test system is only 1.11 bits per Hz for 16QAM, but more advanced systems will have an efficiency of 3 bits per Hz or greater.

E. Transmitter Diversity

Since this project will focus on the forward link (infrastructure to mobile) it will employ transmitter diversity. Diversity is necessary to achieve high performance in wireless communications. Due to vehicular motion the diversity can often be achieved by sampling the channel at different time instances (time diversity) which is typically implemented with interleaving and coding. Unfortunately a vehicle will often need to transmit while stationary and consequenily since the vehicle does not move, the channel will not change and diversity will not be achieved. Transmitter diversity is one way to achieve diversity even when the link is stationary or moving very slowly.

The type of transmitter diversity used on this project is one in which each transmitter sends the same information sequence only with a slight offset in frequency (typically less than 50 Hz).

If the transmitter antennas are spaced far enough apart the signals from each antenna will produce a different response at the receiver antenna. The frequency offset between the transmitters guarantees that the relative phases of each response will be changing with time and consequently the composite signal will be changing with time. This transmitter diversity technique induces time varying fading on the received signal in the absence of vehicle motion. This produces several advantages: 1) the interleaver depth can be design in a principled fashion, 2) the level of diversity is equal to the number of antennas used in transmission, and 3) while the performance is optimized for the case when the vehicle is stationary, it is not degraded when the vehicle is :in motion.

VI. Demodulator

A. Purpose

The demodulator must incorporate sophisticated signal processing algorithms to recover the transmitted data in the presence of fading. Furthermore, it must be coherent because of the QAM modulation scheme. A block diagram of the demodulator is shown in Fig. 11. The IF modulated signal from the RF receiver is sampled by the A/D board, converted to baseband, match filtered, and sampled at the symbol rate. The pilot symbol assisted modulation (PSAM) fading estimator block extracts the pilot symbols and uses them to form an estimate of the fading process, and the deinterleaver reconstructs the coder frame. At the output of the deinterleaver the noise is uncorrelated. The FEC decoder uses soft decoding to correct errors in the symbols, which are finally converted to bits and fed to the DRS for statistical analysis.

The entire demodulator including the DRS is being implemented in the Signal Processing Worksystem (SPW). SPW is a graphical communications design package with an extensive library of communications blocks and powerful analysis tools that aid in determining system performance.

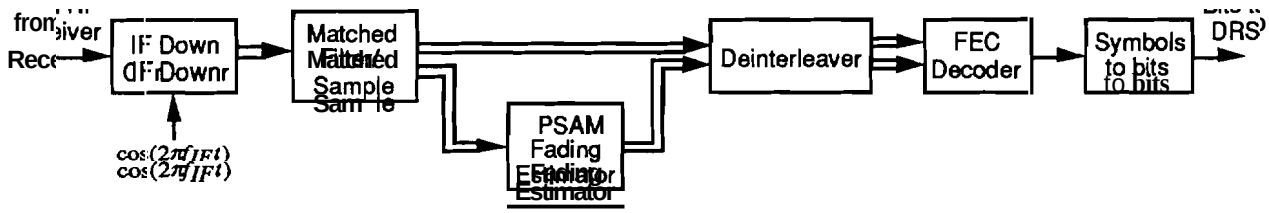

Fig. 11. Demodulator block diagram

B. Symbol and Frame Synchronization

Optimum symbol decisions can be made if the matched filter output is sampled at the appropriate time instant (see Fig. 11). The process of estimating when to sample this filter output is known as symbol synchronization, and is typically accomplished directly from the received signal. Since the input signal will be sampled at a fixed rate, the symbol synchronization consists of two components as seen in Fig. 12: 1) estimation of timing phase and 2) interpolirtion. Designs for interpolators are well established and since the receiver for this project use:; significant oversampling (somewhere between 8-25 times) we will be able to use a

simple first or second order interpolator. This type of interpolator minimizes the complexity while producing an insignificant degradation.

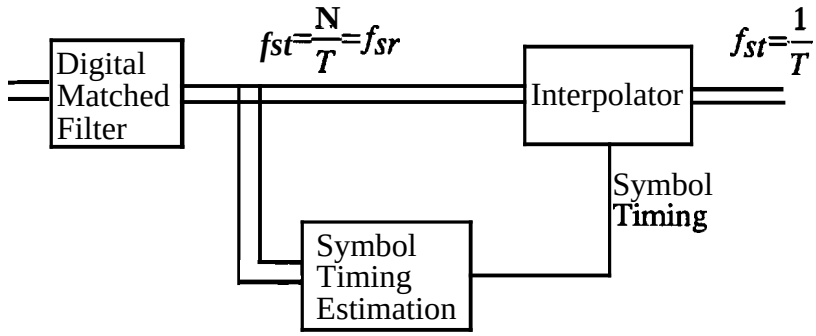

Fig. 12. Symbol synchronization system. This is a detail of the *matched filter/sampler* block in Fig. 11.

The design of the phase estimator is not finalized yet but will follow stantlard practice. We are currently investigating the tradeoffs between open loop and closed loop symbol synchronization techniques. The open loop techniques (e.g., the digital filter and square [2]) offer faster acquisition and a performance optimized for digital circuit implementation, but the loop's performance with large signal constellations being considered in this project has not been reported in the literature. The closed loop techniques like the filter and square loop and the transition tracking loop [3-6] are the more traditional approaches and offer a simpler implementation. A focus of the remainder of this project will be optimizing both of these algorithms for large constellations and the narrowband wireless communication channel and selecting the one providing the best tradeoff in performance and complexity.

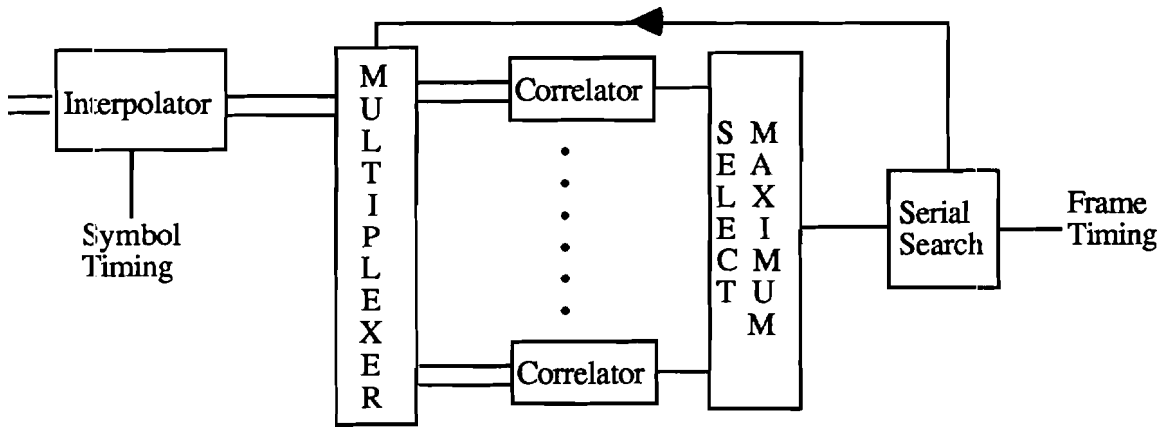

Fig. 13. Frame synchronization architecture

The frame synchronization algorithm will use a combination of a standard parallel correlation detector and a serial search strategy to achieve the desired frame alignment. Figure 13 is the block diagram of this architecture, which was chosen because it provides a desirable combination of rapid acquisition achievable with parallel search strategies and low complexity achievable with serial search strategies. The frame uncertainty can be broken up into N_b blocks and for a given block the multiplexer/correlator combination tests all phases within this block and finds the

maximum correlator output. The phase corresponding to the maximum and the corresponding correlator output value is then passed to the serial search procedure. This serial search procedure uses several consecutive outputs to decide if a lock is obtained. If lock is not declared, then the serial search moves on to the next block in the frame uncertainty and repeats these steps. This search procedure is continued until a lock is obtained. This search procedure is much like that used in pseudo noise code acquisition systems in spread spectrum communication systems. A significant task in the remainder of the project is the optimization of the design of the correlator and the serial search strategy to the land mobile wireless communications channel.

C. PSAM Demodulation

The main purpose of the pilot symbols is to sample and form an estimate of the channel fading to achieve coherent demodulation. The fading process is modeled by a bandpass random process which multiplies the signal. An estimate of this multiplicative distortion is constructed by applying a lowpass interpolation filter to the samples acquired from the pilot symbols. A Wiener filter is used for this since it minimizes the mean squared error of the estimate.

Figure 14 shows a detail of the **PSAM** Fading Estimator block from Fig. 11. The symbol stream is split into the pilot symbol stream and the data stream. The received pilot symbol sequence is normalized by the actual pilot symbol sequence, leaving only the multiplicative distortion. The Wiener filter interpolates these samples of distortion to construct an estimate of the distortion at every symbol period. The data stream must be delayed to compensate for the delay of the Wiener filter.

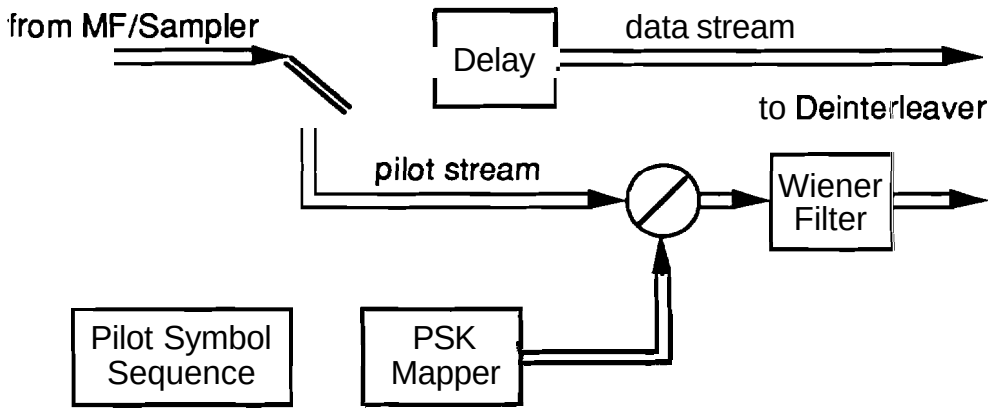

Fig. 14. PSAM Fading Estimator

D. Decoding Architecture

The initial decoding architecture will use maximum likelihood decoding algorithms optimized for the fading channel. This technique will minimize the probability of block error. The inputs to the decoder will be the deinterleaved matched filter outputs and the channel estimates produced by the **PSAM** demodulator. These inputs and the code structure will permit a computation of the posterior mass function of each transmitted codeword, allowing the most likely codeword to be chosen for demodulation. For the higher complexity coding schemes

complexity reduction schemes will be implemented. For example, the 4/7 rate code with 64QAM modulation has over 16 million possible codewords, so an exhaustive search over this large of a set of codewords is not desirable. A thresholding technique like that proposed in [7, 8] will be implemented to reduce the complexity to a manageable level.

Further studies in decoding strategies will be conducted to obtain the best cost versus complexity tradeoff. A strategy which offers significant promise is that of combined hard decision and erasure decoding. In this scheme the demodulator would make standard PSAM hard decisions [9] unless the decisions were perceived to be unreliable and then an erasure would be declared. The reliability of the decision could be measured using the magnitude of the channel estimate produced in the PSAM fading estimator. Combined erasure and hard decision decoding is much simpler and a vast theory exists on the efficient implenlentation of these decoders [1, 10].

VII. Supporting Analysis

A. General

The characteristics of the wireless radio channel which make it difficult to use to communicate are produced by the motion and multipath transmission characteristics. Figure 15 is an example of the typical land mobile communication scenario. Radio waves can propagate via more than one path from the transmitter to the receiver, and each path has a different amplitude and phase. If the transmitter or receiver is in motion then the phase of each path (which is proportional to the propagation delay) will be varying with time:. In narrowband communication these different paths will combine to produce a time varying amplitude. A good example of this time varying signal amplitude is seen in Fig. 16. This time varying carrier amplitude is commonly referred to as signal fading. This fading signal characteristic of land mobile channels is the predominant impairment for narrowband wireless communications.

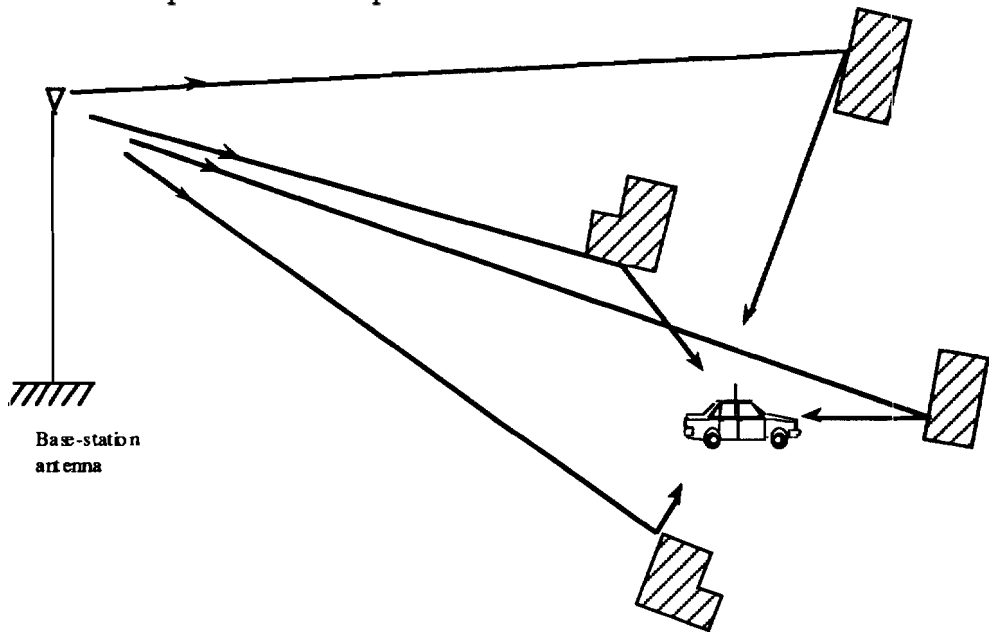

Fig. 15. A typical land mobile communication scenario

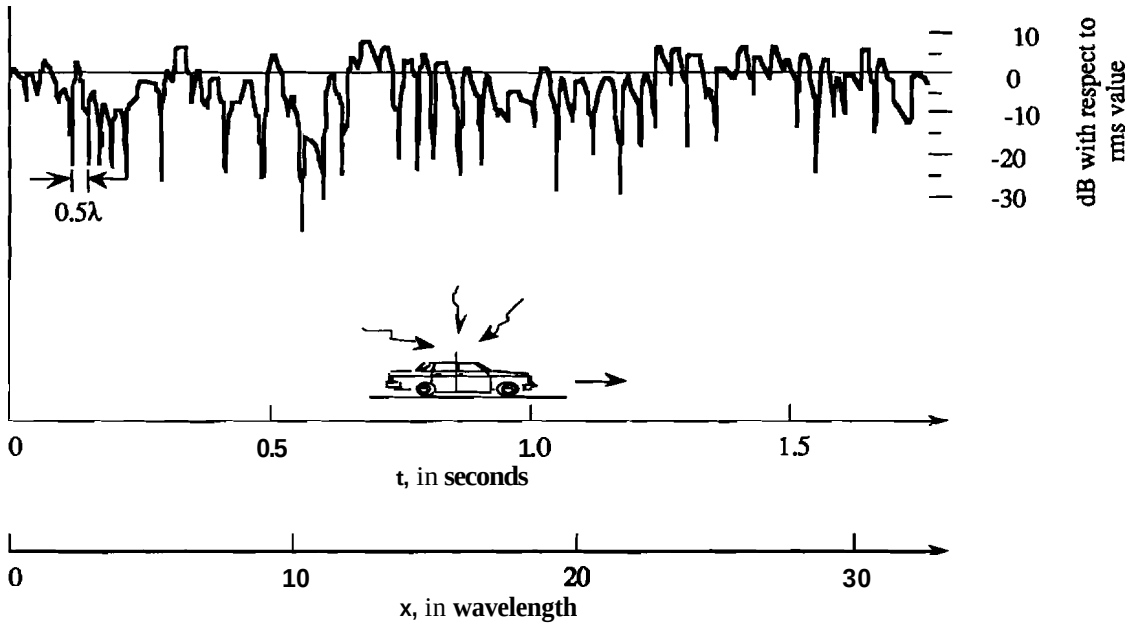

Fig. 16. An example of time varying signal fading

A-1. Channel Parameters

The multiplicative fading distortion seen Fig. 16 is caused by the multipath propagation and the motion of the vehicle. A land mobile wireless communication system must be designed for the worse case conditions and the lowest signal to noise ratio is produced when no line of sight propagation path exists between the infrastructure and the vehicle. The best model for the fading process in channels with no line-of-sight path is that the amplitude follows a Rayleigh envelope (in-phase and quadrature components of the channel response are Gaussian). Propagation paths which are from the direction in which the vehicle is traveling will experience a positive Doppler frequency shift and conversely the paths from behind the vehicle will experience a negative Doppler frequency shift. Consequently the bandwidth of the fading process is usually $2f_D$, where f_D is the maximum Doppler shift produced by the vehicle motion. The Doppler frequency f_D is dependent on the carrier frequency and the speed of the vehicle as $f_D=v/\lambda=vf_C/c$, where v is the speed of the vehicle and $c=3\text{x}10^8$ m/s is the speed of light. For this communications link, $f_C\approx220$MHz. A vehicle driving at 75mph (33.5 m/s) would experience a Doppler shift of 24.6Hz, whereas a vehicle driving at 100mph (44.7 m/s) would experience a Doppler shift of 32.8Hz.

A common analytical model which represents an average narrowband channel is called the isotropic scattering, Rayleigh fading channel model [11]. This channel model will be used for algorithm design and computer verification of the different components of the communication system. The power spectrum of the fading process is given in Fig. 17. This spectrum is bandlimited to $2f_D$ and the performance of a narrowband digital communication system is usually parameterized by f_DT.

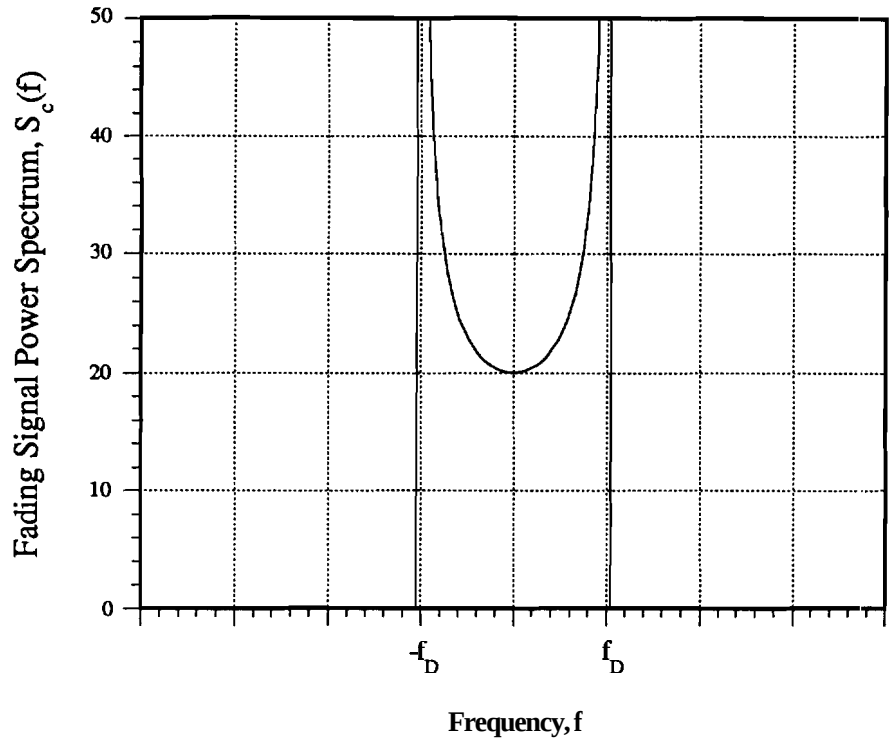

Fig. 17. The spectrum for fading produced by isotropic scattering.

A-2. Diversity in Wireless Digital Communications

In narrowband wireless communication systems performance is dominated by the fading characteristics. In normal operation, the performance is near error free except when deep fades occur and then a burst of errors is induced. Since in the Rayleigh fading channel the probability of a deep :fadeoccumng is still significant even at high signal to noise ratio (SNR), the single channel communication system has a bit error probability (BEP) which is inversely proportional to the SNR, i.e.,

$$P_B(E) \propto (SNR)^{-1}$$

This characteristic makes it infeasible to provide a high quality of data service in a single channel type system. The traditional digital communication technique which provides the necessary performance is the use of diversity. Diversity implies that multiple copies of an information bit is transmitted or received over different fading channel responses. When L_d :levelsof diversity are used in a digital communication system the resulting bit error probability has the characteristic

$$P_B(E) \propto (SNR)^{-L_d}$$

Figure 18 shows the BEP curves for L_d=1,2, 4 for 16QAM modulation in the Rayleigh fading channel. Note that the desired BEP performance (10^{-5}) can be achieved at a reasonable SNR with an $L_d \geq 3$ so the goal in this project is to produce a design which attains at least 3 levels of diversity.

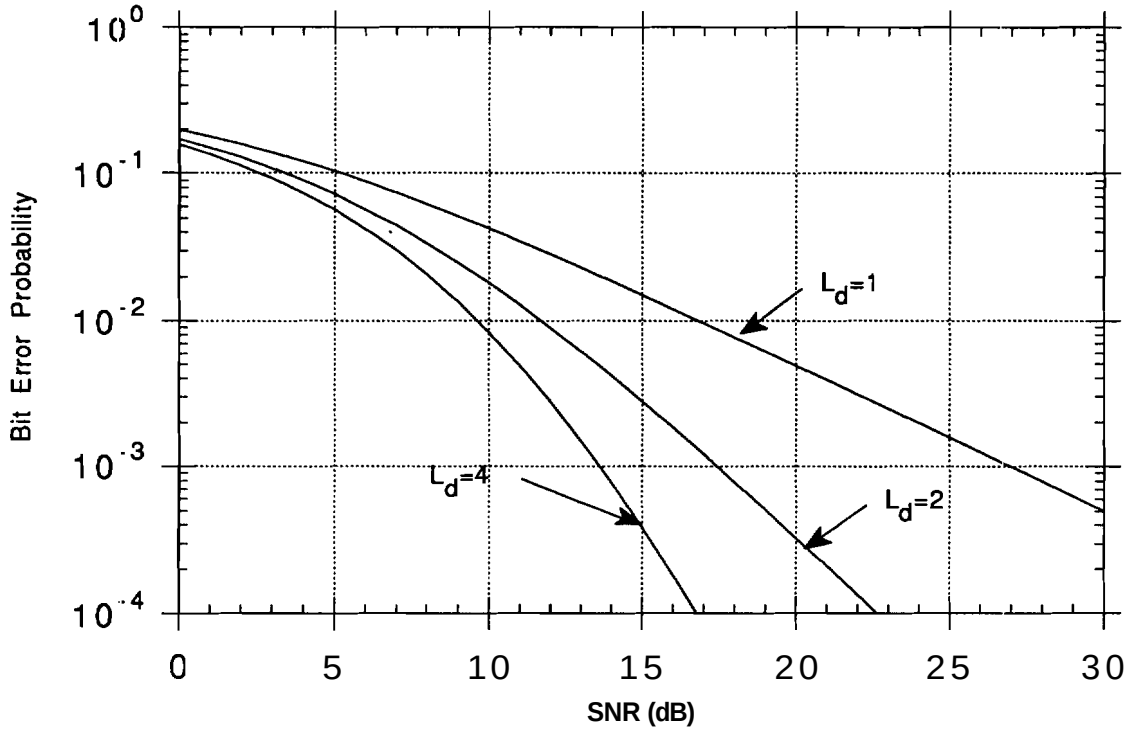

Fig. 18. The bit error probability versus SNR parameterized by the number of diversity levels. Coherent demodulation of 16QAM signals in Rayleigh fading.

B. Link Budget

Table 2 is a link budget for the architecture being built in this project. Note to achieve a 2km communication range we can accommodate over 35 dB of excess path loss compared to free space propagation. This number compares favorably with that typically measured in propagation studies at other frequencies [11].

Table 2. Link budget

Parameter	Value
Output RF Power	10 dBm
TX Antenna Gain	3 dB
EIRP	13 dBm
Propagation Constant $(\lambda/4\pi)^2$	-19.3 dB
Propagation Loss - Free Space (d^2)	-99dB (d=89 kilometers)
Propagation Loss - Heavy Urban (d^3)	-99dB (d=2000 meters)
Propagation Loss - Upper Bound (d^4)	-99dB (d=300 meters)
RX Antenna Gain	3 dB
Received Signal Power, P_r	-102.3 dBm
E_b (P_rT/m)	-144.3 dBm/Hz (T=4000Hz, m=4)
Thermal Noise Spectral Density	-174dBm/Hz
Noise Figure	6dB
Receiver Noise PSD level, N_0	-168dBm/Hz
E_b/N_0 needed to achieve a BEP=10^{-5}	22dB
E_b needed to achieve a BEP=10^{-5}	-146dBm/Hz
Link Margin	1.7 dB

C. Pulse Shape Design

The same pulse shape is used for all symbols, so the bandwidth of the transmitted signal is equivalent to the bandwidth of the pulse. In order to obtain a signal with a narrow bandwidth, the pulse needs to be very wide in time. However, if the pulse has a long period, the throughput will be unacceptably low. The solution to this problem is to allow the symbol pulses to overlap, so that each pulse is wide in time and has a narrow bandwidth, yet the throughput remains high. Using this format, the symbol period is defined as the time between successive pulses, so each pulse is actually longer than one symbol period. Unfortunately, since the pulses overlap inter-symbol interference (ISI) will result unless the pulses are carefully designed.

The well known Nyquist Criterion for zero ISI states that if the autocorrelation of the pulse shape is zero at all multiples of the symbol period then no ISI will occur. There are several common pulses that satisfy this criteria, such as the Raised Cosine Pulse. In practice these pulses do have a small amount of ISI, and the frequency response is quite good. Another pulse which satisfies Nyquist's condition was designed by Mueller [12]. This pulse exhibits zero ISI and also has very good frequency characteristics, so it was chosen for use in this system.

The autocorrelation function for the zero ISI pulse is shown in Figure 19 for 27 samples per symbol and a pulse 25 symbol periods long. The frequency response for this pulse and a pulse

with 30 samples per symbol is shown in Figure 20, along with the FCC 4kHz spectral mask. It may be seen that either of these pulses fit within FCC regulations. For f_{St}=100kHz and N_{St}=27, the symbol rate is R_{St}=3704 symbols per second, giving a spectral efficiency of 92.6%.

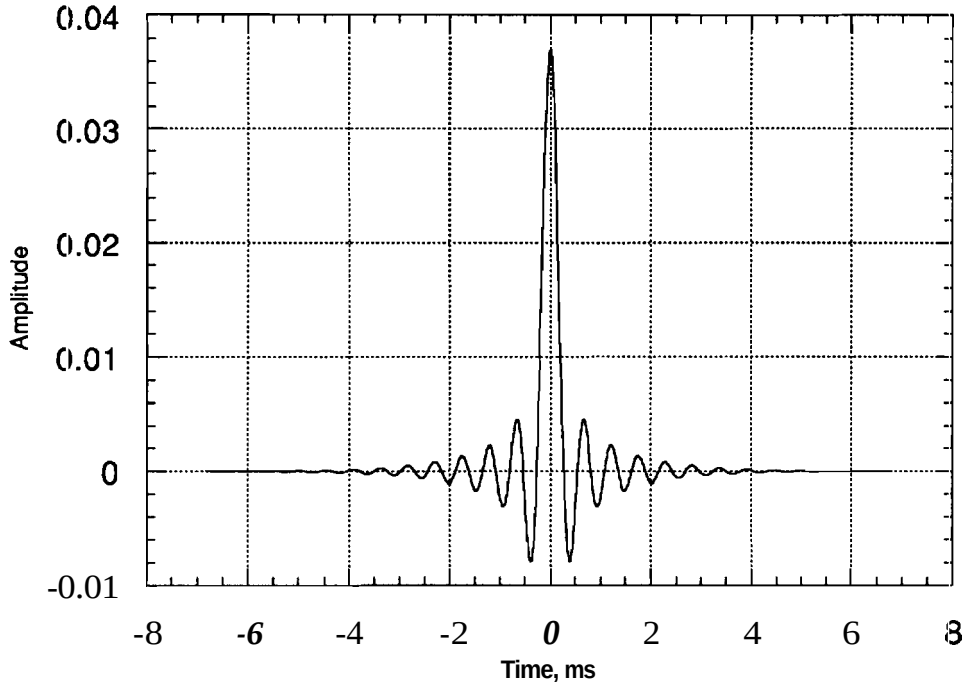

Fig. 19. Autocorrelation for Zero ISI Pulse: N_{St}=27, pulse is 25 symbol periods long.

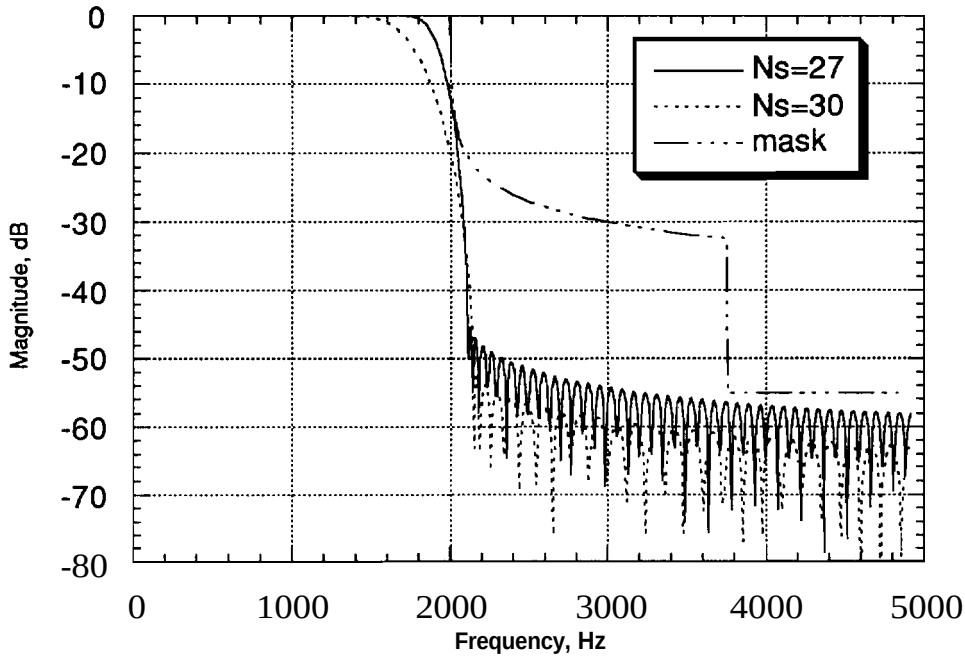

Fig. 20. Frequency Response of Zero ISI Pulses 25 symbol periods long.

D. PSAM Demodulation

As described earlier, the multiplicative distortion is a bandpass ranclom process with bandwidth equal to the Doppler frequency f_D. By Nyquist's Sampling Theorem, the minimum sampling :rate that will recover this bandpass process is $2f_D$. Since the symbol rate is IIT, the channel must be sampled every $1/(2f_DT)$ symbols. Hence, there can be at most $1/(2f_DT)$ symbols between 2 adjacent pilot symbols, i.e. $(N_p-1)\leq 1/(2f_D)$.

In this system, Doppler frequency is about 33 Hz for the worst case, and the symbol rate IIT is about 3000 Hz so the maximum pilot symbol spacing is $N_p\leq 45.5$. To achieve better resolution and provide some noise tolerance, $Np=9$ is selected.

In the Raleigh fading channel the received signal is distorted by both multiplicative noise and Additive White Gaussian Noise (AWGN). The relation can be expressed as:

$$r(t)=c(t)x(t)+n(t),$$

where $r(t)$ is the received signal, $c(t)$ is the multiplicative noise, $x(t)$ is the transmitted signal, and $n(t)$ is the AWGN. The multiplicative noise is estimated by passing the samples of $r(t)$ which correspond to the pilot symbols through the Wiener filter. The estimate of the channel distortion can be divided out of the received signal to recover the transmitted signal as:

$$r(t)/\hat{c}(t)=x(t)+n(t)/\hat{c}(t)$$

Alternatively, sophisticated decoding algorithms can be used to remove the distortion even more effectively.

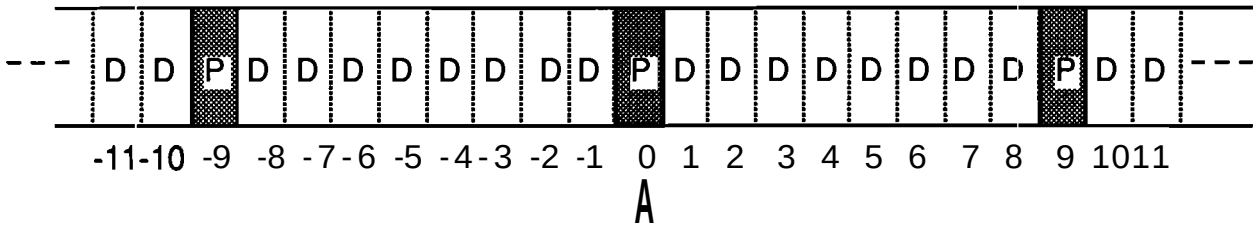

Fig. 21. Filter Window

For $N_p=9$, Figure 21 shows the frame structure of the Wiener filter. The zeroth time instant is arbitrarily chosen to lie on a pilot symbol. To estimate the channel distortion for the data samples -4 to +4, a noncausal filter spanning $K=16$ pilot symbols (indices -72,-63,..., -9,0,9,...54,63) is used. The channel estimate is formed via

$$\hat{c}(k)=\sum_{i=-\lfloor K/2\rfloor}^{\lfloor (K-1)/2\rfloor} h^*(i,k)r(iN_p),$$

where:

$h(i,k)$ are the Wiener filter coefficients

and k=-4 to +4 for this example.

The Wiener filter coefficients are calculated from the Wiener-Hopf equation

$$\mathbf{R}\mathbf{h}(k)=\mathbf{w}(k).$$

where:

$\mathbf{h}(k)=[h(-\lfloor K/2\rfloor,k),h(-\lfloor K/2\rfloor+1,k),\ldots,h(\lfloor (K-1)/2\rfloor,k)]^t$,

$\mathbf{R}=E[\mathbf{r}\mathbf{r}^{t^*}]$,

and $\mathbf{r}=[r(-\lfloor K/2\rfloor N_p),r((-\lfloor K/2\rfloor+1)N_p),\ldots,r((\lfloor (K-1)/2\rfloor)N_p)]^t$

The equations for the correlation functions for the Rayleigh fading channel were determined to be [9]

$$R_{ik}=\gamma_b m(N_p-1)\frac{q}{q+1}\tilde{R}_C((i-k)N_pT)+\delta_{ik}$$

$$w_i(k)=\gamma_b\frac{m(N_p-1)}{\tilde{b}^*}\frac{q}{q+1}\tilde{R}_C((iN_p-k)T)$$

where:

γ_b is ihe signal noise ratio,

q is the ratio of pilot power to data power,

m is the number of bits per symbol, and

$\tilde{R}_C(\tau)=\exp(j2\pi f_O\tau)J_O(2\pi f_D\tau)$ is the normalized multiplicative noise autocorrelation function.

The frequency response of Wiener's filter is shown below for K=16 and K=64.

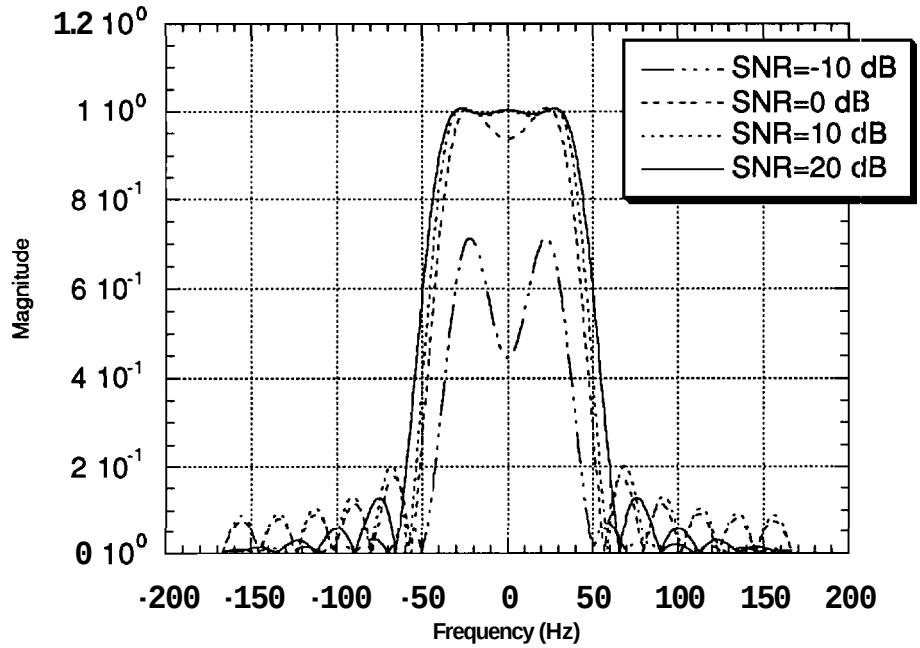

Fig. 22. Wiener Filter Response, K=16, N_p=9

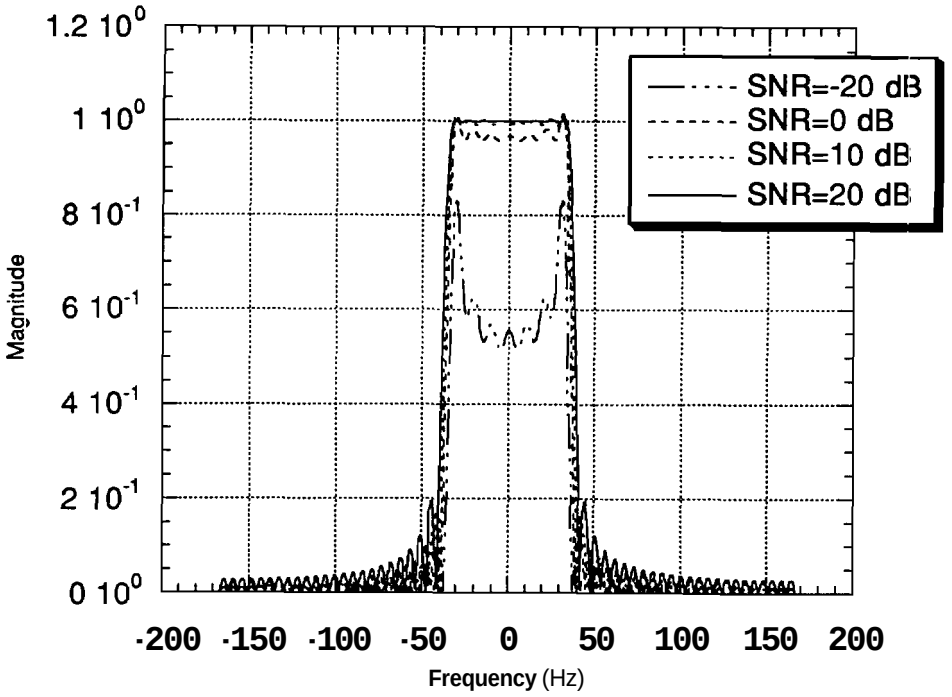

Fig. 23. Wiener Filter Response, K=64, N_p=9

E. Transmitter Diversity

This section overviews the analysis done on the transmission diversity scheme proposed for this project. The details can be found in [13] and have been submitted as a regular paper in the IEEE Transaction on Vehicular Technology. The essential idea in this scheme is that with transmitter diversity the signal will not likely stay in a deep fade for a long period of time and the signal has well characterized time variations. These two characteristics allow principled interleaving and coding strategies to be designed and implemented. Three levels of diversity will achieve the desired performance, consequently we use three antennas. The antennas are traditional 5/8 wave dipoles and provide about 5dB of gain over isotropic radiation. Figure 24 shows the geometry of the proposed antenna configuration for this project.

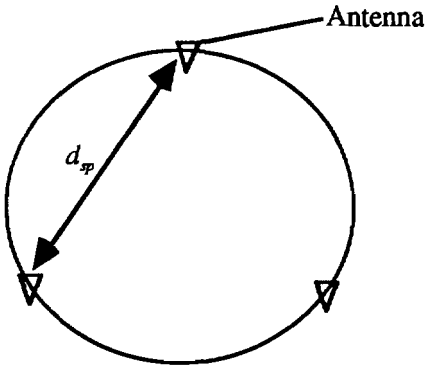

Fig. 24. Transmitter antenna geometry

E-1. Fading Statistics

The complex analytical transmitted signal at the ith antenna has the following form

$$s_i(t) = z(t)e^{j2\pi f_i t}$$

where $z(t)$ is the complex envelope of the modulation and f_i is the frequency offset from the carrier imposed on the ith antenna. The frequency offset on each of the antennas is what produces the controlled time-varying characteristics at the receiver that we desire. The resulting baseband equivalent multiplicative distortion (MD) process at the receiver is then

$$c(t)=C(t)e^{j\chi(t)}=\frac{e^{-j2\pi f_o t}}{\sqrt{L_d}}\sum_{i=0}^{L_d-1} c_i(t)\exp\left[j\frac{4\pi f_O i t}{L_d-1}\right]$$

$c_i(t)$ represents the independent Rayleigh fading process for the propagation between the ith antenna and the receiver, and $2f_O$ is the bandwidth expansion of the transmitter diversity system. Again we assume that each transmitting path is accurately modeled by independent isotropic scattering. For cases of particular interest, the autocorrelation of the MD process $c(t)$ is then

$$R_c(\tau)=\frac{1}{3}E_b J_0(2\pi f_D\tau)\left[1+2\cos(2\pi f_o\tau)\right],\ \text{if } L_d=3.$$

Notice that the difference in the autocorrelation of the MD process for systems using transmitter diversity or not is the terms $\cos(2\pi f_o\tau)$ which provide the enforced time-varying fading effect. Also note if the intentional frequency offset is not used ($f_O=0$), then the autocorrelation of MD reduces to that discussed in Section VII-A.

Ideal interleaving (independent fading on each code symbol) provides the best performance with coded modulations. This condition implies that the autocorrelation of the MD samples at any two code symbols be equal to zero, i.e.,

$$\text{Ideal Interleaving} \Leftrightarrow E\left[c_k c_l^*\right]=E_b\delta_{k-l}$$

where k and 1 are any two time indexes of a transmitted codeword. If transmititer diversity is not used, then in a very slow fading situation (i.e., f_D is close to zero), the autocorrelation of the MD process remains at a value close to E_b for large values of τ and ideal interleaving cannot be achieved in this case unless a very large buffer in the receiver can be used and a long processing delay is tolerable.

The transmitter diversity technique using intentional frequency offset provides a practical solution for providing independent fading. Figure 25 illustrates the autocorrelation function (normalized to E_b) of the MD process for various transmitter diversities (multiple antennas) in a stationary fading ($f_D=0$) situation. Two features can be observed from Fig. 25. First, the autocorrelation function of the MD process drops quickly as a function of normalized time, $f_o s$. Second, the more antennas we use, the longer in normalized time the autocorrelation goes before it returns to the highly correlated areas (± 1). Consequently using more antennas can generate more zero crossing points in the autocorrelation of MD before it goes back to the highly correlated areas (± 1). Since we place the tones (offset frequencies for different antennas) with uniform separation in the frequency spectrum over a fixed bandwidth these zero crossing points are also uniformly separated (periodic) to the extent of L_d (space diversity). This property is very significant since 1) the most prevalent interleaver uses an array processor which produces

the uniformly interleaved codeword and 2) to provide near ideal interleaving requires the correlation of MD be zero at the displacement of any multiples (up to a certain extent) of the interleaving depth (D_{iv}).

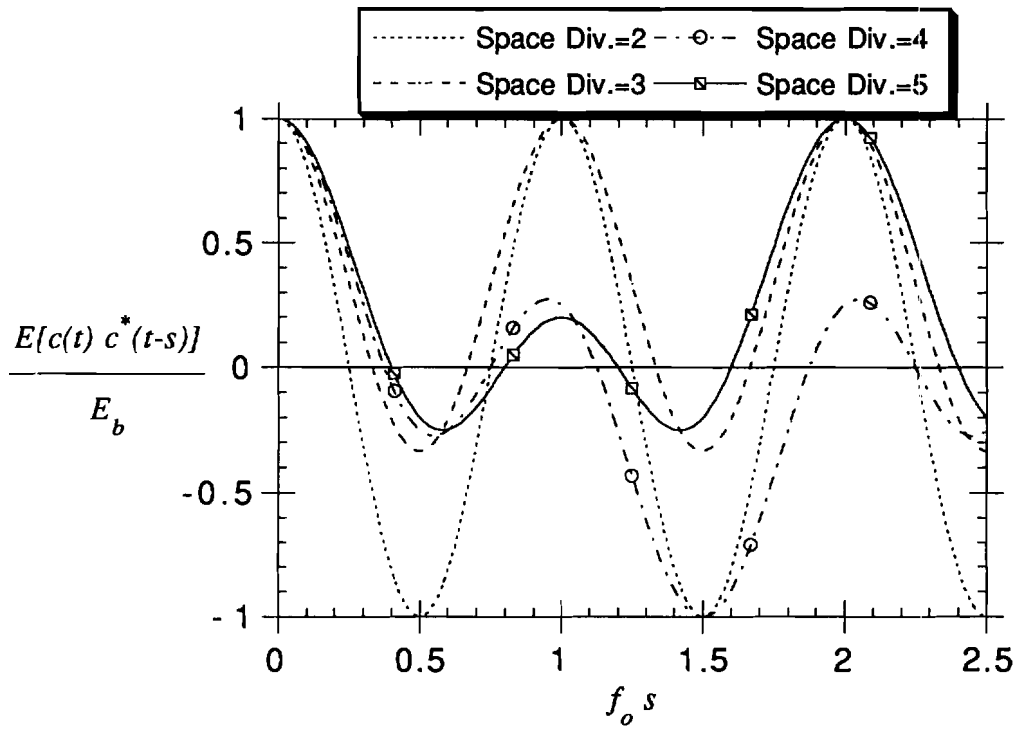

Fig. 25. Autocorrelation of the MD process in stationary fading.

E-2. Error Performance

Using the second order statistics highlighted in the previous section bit error probability (BEP) expressions can be obtained to characterize the performance as a function of average SNR. Again the details of the results are given in [7]. Figure 26 shows the effect on bit error probability of a R=1/3 16QAM code by using frequency offset with varying interleaving depth in stationary fading (f_D=0) and γ_b =14.65 dB. PSAM with N_p=7, a Wiener filter of length 12 and f_oT=0.005 are considered. The optimal points of $f_oD_{iv}T$ (which yield the lowest BEP) for space diversity=3 and 4 are 113 and 318 respectively.

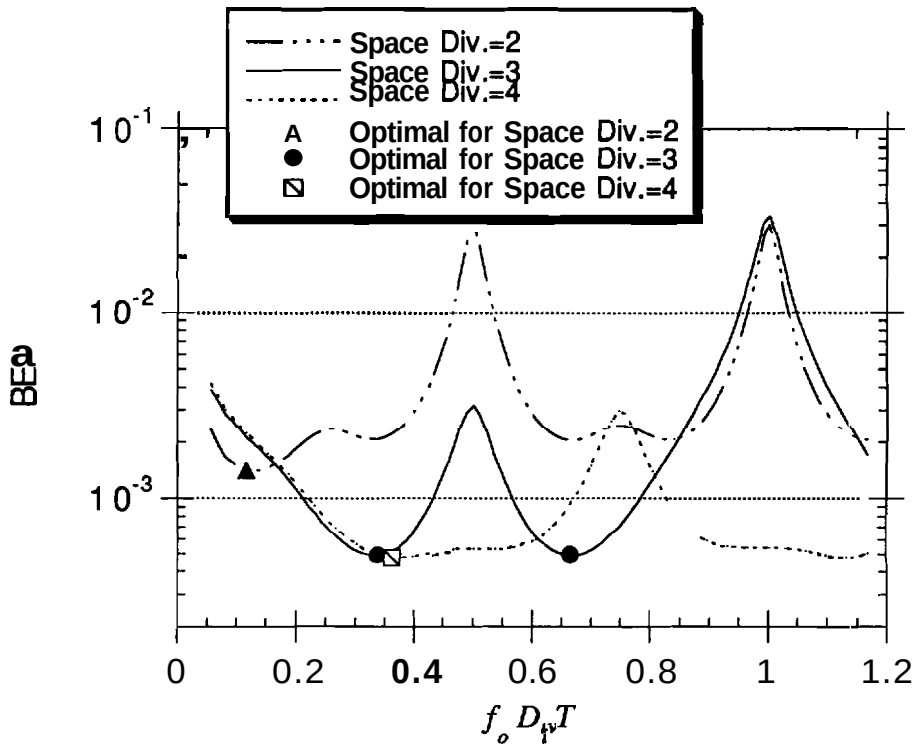

Fig. 26. The **BEP** of a R_C=1/3 16QAM code versus frequency offset and interleaving depth product in stationary fading. **2D-PUB, SNR=14.65dB,** N_p=7, $2K$=12.

E-3. Antenna Geometry

We have also characterized the **BEP** performance as a function of the antenna geometry. This analysis uses the propagation characteristics of a wireless channel to get an estimate of the performance as a function of antenna geometry. This performance analysis will be documented in a future paper by Dr. Kuo and Prof. Fitz. Figure **27** is a plot of **BEP** versus antenna spacing in the geometry given in Fig. **24.** This figure demonstrates that near ideal interleaving performance can be achieved with an antenna spacing as small a two wavelengths **(3** meters for this ITS application)

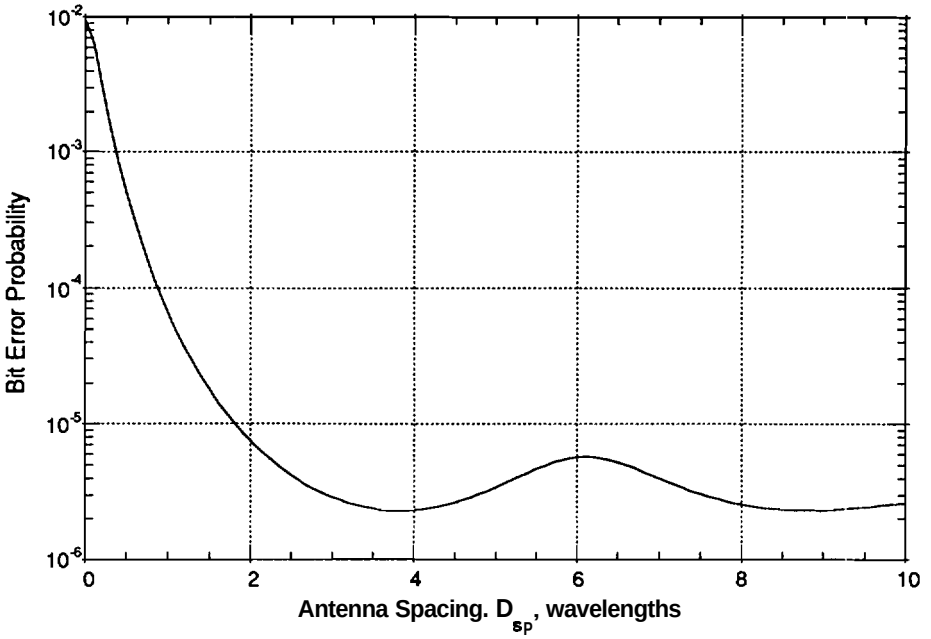

Fig. 27. BEP versus antenna spacing. SNR=20dB, f_oT=0.005, f_DT=0.

F. Modulation Format

Section V-C introduced several constraints on the system parameters which arose from the frame structure. If those constraints are met, there will be an integer number of symbols in every frame, and the coder and interleaver will be synchronized to the pilot symbols. However, there are additional constraints imposed on these parameters due to the mathematical models of the system and the equipment used to build the system. Most of these have been discussed in previous sections, and they are summarized here for use in selecting the final system parameters.

The sampling frequency of the DSP board may be selected from 100kHz, 48kHz, or 44.1kHz. In order to achieve the highest oversampling and best pulse shape, the sampling rate of the transmitter is chosen to be f_{st}=100kHz. The number of samples per symbol N_{st} must be an integer. These two parameters specify the symbol rate $R_S=f_{st}/N_{st}$. Obviously the symbol rate should be as high as possible, and it was determined that the highest symbol irate that fits under the FCC spectral mask is for N_{st}=27, R_S=3.704kHz.

Analysis performed on the UW determined that to achieve a probability of false alarm of 10^{-8} and a probability of detection of 0.99 in the presence of fading with a symbol error rate of $P_S(E)$=0.1, the UW must be 85 bits long.

To achieve ideal interleaving, the following relationship must be satisfied:

$$f_oD_{iv}T=\frac{L_d-1}{2L_d}$$

where:

f_o :is the frequency offset,

T is the symbol period, and

L_d is the number of levels of diversity (antennas)

Recall that 3 antennas are being used, and as stated above R_S=3.704kHz, so $T=1/R_S=0.00027$ and $f_O=1/(0.00081D_{iv})$. The transmission bandwidth of the signal will be proportional to $1/T+f_O$, so it is desirable to have f_O relatively small; $f_O \leq 50$Hz should suffice. Additionally, $D_{iv}L_{CO} \leq 1024$ due to memory constraints on the DSP board.

The multiplicative distortion is a bandpass random process with bandwidth f_D. For the design of this system a worst case Doppler frequency of f_D=33Hz was used. At a worst case symbol rate of 3000 symbols per second, $f_DT=0.011$, and $N_p \leq 45.5$.

Summary of Constraints

f_{st}=100kHz N_{st}=27 R_S=3704sps $L_{uw_{bits}}$=85 bits

$\frac{L_{f_{DGS}}}{L_{ci}}$=integer $\frac{L_{f_C}}{D_{iv}L_{CO}}=\frac{L_{f_{DGS}}/R_C}{D_{iv}L_{CO}}$=integer $\frac{L_{f_C}}{(N_p-1)}=\frac{L_{f_{DGS}}/R_C}{(N_p-1)}$=integer

$\frac{(N_p-1)}{L_{CO}}$=integer $\frac{(N_p-1)T_p}{D_{iv}L_{CO}}$=integer $N_p \leq 45$ $f_O=\frac{1}{0.00081D_{iv}}$

$D_{iv}L_{CO} \leq 1024$ D_{iv}/L_{CO}=integer $f_O \leq 50$Hz

G. Data Generation and Recovery Systems

1. Data Recovery System

The Data Generation System (DGS) produces and transmits the Unique Word (UW) followed by the User Frame (UF), repeating this sequence indefinitely. Analysis determined that the UW should be 85 bits long. The UF is 10 times longer than the UW, or 850 bits, providing a channel efficiency of 91%.

The DGS has two outputs. The first output is the information word which consists of a parallel output of 2 to 6 bits of the UW and UF. The second output is a synchronization clock, called the symbol rate clock, such that the information word is valid on the rising edge of the symbol rate clock. The DGS supports symbol clock rates up to 20 kHz.

2. Data Recovery System

The Data Recovery System (DRS) reads the information word on the rising edge of the symbol rate clock. The system begins by searching for a UW to establish synchronization. When a UW is found, the system will look for another UW 850 bits after the end of the first one. The data between the two UW is the UF. If both UW are detected, the DRS assumes synchronization has been established and the UF will be analyzed for errors. If both UW are not detected in the appropriate places, the data will assumed to be invalid. The system will then search for a new UW at all positions in order to re-establish synchronization.

The DRS has three outputs: the Error Count, the Block Validation Clock, and the Demodulation Validation Flag. The number of errors will be outputted on the rising edge of the Block Validation Clock. Since it is possible to have 850 errors, 10 bits of accuracy are required. The Error Count is an 8 bit serial output with two write cycles. The Demodulation Validation Flag shall be set whenever the DRS finds a UW at the beginning and end of a UF.

3. Uniaue Word

The DGS and DRS are designed to maintain synchronization even in the presence of a high symbol error probability (SEP). The design criteria is that for a SEP of 0.1, the Probability of false alarm (P_F) is less than or equal to 10^{-8}, and the probability of detection (P_D) is greater than or equal to 0.99. The P_F is the probability that part of the UF is mistaken as the UW, and the P_D is the probability that the UW is correctly recognized.

It is impossible to meet both these constraints for a SEP of 0.1 unless the UW is recognized even though some errors have occurred. Since a certain number or more bits of the UW are required for proper detection and not misdetected as a false alarm, the random bits which formed the UW follow a binomial distribution:

Binomial Distribution

$$P_n(k)=\left(\frac{n!}{k!(n-k)!}\right)p^k q^{n-k}$$

n = length of Unique Word
k = length of Unique Word - number of Errors allowed
p = probability of getting occurrence
q = 1-p

For the probability of detection, the probability of getting an occurrence is the probability of getting a UW bit. So, p=1-P(b) and q=P(b). The probability of a bit error and the probability of detection is shown below. In the probability of a bit error, M is the number of modulation scheme levels, $M=2^m$.

Probability of A Bit Error

$$P(b)=P(b|s)P(s)$$

$$P(b|s)=\frac{M}{2M-2}$$

$$P(s)=0.1$$

$$Pn(k)=\sum_{l=k}^{n}(n,k)(1-P(b))^l(P(b))^{n-l}$$

For the probability of false alarm, the probability of getting an occurrence is getting one bit of the UW to match one bit of the UF. So the probability of getting an occurrence is one half. So, p=1/2 and q=1/2. The probability of false alarm is shown below.

$$Pn(k) = \sum_{l=k}^{n} (n,k)(0.5)^n$$

From these two equations it was determined that for a UW 85 bits long, ;allowing16 errors yields $P_F = 2.62013 * 10^{-9}$ and $P_D = 0.99586$ with a modulation scheme of one bit, and $P_D = 0.99999$ with a modulation scheme of six bits. Simulations were run to verify these results. For 4000 :symbols per second and a 16QAM constellation, it would take approximately 67 days for a false: alarm to occur. For this reason the design was tested for lower P_F values, and it is assumed that since these results matched, the analysis for $P_F \leq 10^{-8}$ should also be correct.

VIII. Conclusions

This report has provided an overview of the ITS project which develops a new paradigm in bandwidth efficient land mobile communications. The project develops a recursive model based modulation scheme which is optimized for the use of transmitter antenna diversity, forward error control coding, pilot symbol modulation, and the statistical characteristics of the received signal. Furthermore, the architecture necessary for actual field tests is implemented.

The current status of the project is as follows: The design phase is nearly completed. A theoretical. analysis has shown the existence of several possible modulation schemes, in terms of codes and signal constellations, that attain at least 3 bits/Hz bandwidth efficiency at 10^{-5} BEP. The baseband modulator has been constructed using a Motorola 56002 DSP and is undergoing verification. The baseband demodulator is partially completed in the Signal Processing Worksystem and is also undergoing verification.

Due to its flexibility, the system not only opens the door for even higher bandwidth efficient communication systems, but it also will serve as a testbed for further research. This work will hopefully stimulate interest in utilizing the frequencies allocated to the ITS program.

IX. References

[1] S. Lin and D. Costello, Error Control Coding, Prentice Hall, Englewood Cliffs, NJ, 1983.

[2] M. Oerder and H. Meyr, "Digital Filter and Square Timing Recovery," IEEE Trans. Commun., vol. COM-36, May 1988, pp. 1988.

[3] F.M. Gardner, "A BPSK/QPSK Timing Error Detector for Sampled Receivers," IEEE Trans. Commun., vol. COM-34, May 1986, pp. 423-429.

[4] L.E. Franks, Synchronization Subsystem: Analysis and Design, in Digital Communications, *Satellite/Earth* Station Engineering, K. Feher, Editor. 1981, Prentice Hall: Englewood Cliffs, NJ.

[5] E.A. Lee and D.G. Messerschmitt, Digital Communications, Kluwer Academic Publishers, Boston, 1988.

[6] W.C. Lindsey and M.K. Simon, Telecommunications Systems Engineering, Prentice-Hall, Englewood Cliffs, NJ, 1973.

[7] J.P. Seymour and M.P. Fitz, "Near-Optimal Symbol-by-Symbol Demodulation Algorithms for Flat Rayleigh Fading," IEEE Trans. Commun., 1995,

[8] J.P. Seymour, "Improved Synchronization in the Mobile Communications Environment," Purdue University, 1994.

[9] J.K. Cavers, "An Analysis of Pilot Symbol Assisted Modulation for Rayleigh Faded Channels," IEEE Trans. Veh. Technol., vol. VT-40, November 1991, pp. 686-693.

[10] J.G. Proakis, Digital Communications, McGraw-Hill, New York, 1989.

[11] W.C. Jakes, Microwave Mobile Communications, Wiley, New York, 1974.

[12] K.H. Mueller, "A New Approach to Optimum Pulse Shaping in Sampled Systems Using Time-Domain Filtering," Bell System Tech. Journal, Vol. 52, No. 5, May-June 1973, pp. 723-729.

[13] W.-Y. Kuo, "Architecture Designs for Improving Performance in Fading Channel Communications," Purdue University, 1994.

Appendix A. Summary of Notation

f_{st}	Transmitter Sampling Rate	(100kHz, 48kHz, or 44.1kHz)
T_{st}	Sampling Period at Transmitter	($T_{sr}=1/f_{sr}$)
N_{st}	Number of Samples per Symbol at Transmitter	
R_S	Symbol Rate from DSP board	
T	Symbol Period from DSP board	($T=1/R_S$)
m	Number of Bits per Transmitted Symbol	
M	Size of Modulation Alphabet	($M=2^m$)
E_b	Bit Energy	
P_r	Received Signal Power	
$N0$	Noise Power Spectral Density	
γ_b	Signal to Noise Ratio per bit, $\gamma_b=E_b/N0$	
f_C	Carrier Frequency	
fIF	Intermediate Frequency	
$x(t)$	Transmitted Signal	
$r(t)$	Received Signal	
$c(t)$	Multiplicative Noise	
$C(t)$	Magnitude of c(t)	
$\chi(t)$	Phase of c(t)	
$R_C(\tau)$	Autocorrelation of c(t)	
$J0$	0^{th} order Bessel function	
$n(t)$	Additive White Gaussian Noise	
K	Length of Wiener Filter	
d_{sp}	Separation distance between antennas	
L_{ci}	Code Block Length (input to coder)	
L_{co}	Code Block Length (output of coder)	
R_C	Code Rate (L_{ci}/L_{co})	
N_p	PS Spacing	
T_p	Pilot Symbol Period	
$L_{f_{DGS}}$	Length of DGS Frame	
L_{f_C}	Length of Coded Frame	
L_{f_I}	Length of Interleaver Frame	
$L_{f_{PS}}$	Length of Pilot Symbol Frame	
L_{uw}	Length of the Unique Word	
L_d	Levels of Diversity	
f_D	Doppler Frequency	
f_o	Frequency Offset	
D_{iv}	Interleaving Depth	
v	Velocity of the Vehicle	
c	Speed of Light	
η	Number of bits per Hz (efficiency)	
P_F	Probability of False Alarm	
P_D	Probability of Detection	
$P_S(E)$	Probability of Symbol Error	
$P_B(E)$	Probability of Bit Error	

Abbreviations

A/D	Analog to Digital
AWGN	Additive White Gaussian Noise
BEP	Bit Error Probability
D/A	Digital to Analog
DGS	Data Generation System
DRS	Data Recovery System
DSP	Digital Signal Processor
EIRP	Effective Radiated Isotropic Power
FCC	Federal Communications Commission
FEC	Forward Error Control
IF	Intermediate Frequency
ISI	Inter-Symbol Interference
ITS	Intelligent Transportation System
MD	Multiplicative Distortion
PSAM	Pilot Symbol Assisted Modulation
PSD	Power Spectral Density
PSK	Phase Shift Keying
QAM	Quadrature Amplitude Modulation
RF	Radio Frequency
RU	Receiver Unit
RX	Receiver
SEP	Symbol Error Probability
SNR	Signal to Noise Ratio
SPW	Signal Processing Worksystem
TU	Transmitter Unit
TX	Transmitter
UF	User Frame
UW	Unique Word